




Article

Characterization of Fresh and Cured Properties of Polymer Concretes Based on Two Metallurgical Wastes

Andres Seco ^{1,*}, Angel Maria Echeverría ¹, Sara Marcelino ¹, Benat García ² and Sandra Espuelas ¹

¹ Institute of Smart Cities, Public University of Navarre, 31006 Pamplona, Spain; amecheverria@zabala.es (A.M.E.); sara.marcelino@unavarra.es (S.M.); sandra.espuelas@unavarra.es (S.E.)

² Department of Mining and Metallurgical Engineering and Materials Science, Faculty of Engineering Vitoria-Gasteiz, University of Basque Country UPV/EHU, 01006 Vitoria-Gasteiz, Spain; benat.garcia@ehu.eus

* Correspondence: andres.seco@unavarra.es; Tel.: +34-948-169-682; Fax: +34-948-169-148

Received: 26 December 2019; Accepted: 20 January 2020; Published: 23 January 2020



Featured Application: Authors are encouraged to provide a concise description of the specific application or a potential application of the work. This section is not mandatory.

Abstract: Polyester polymer concretes can substitute conventional concretes based on their usually good mechanical strength, adequate physical properties, and high resistance against aggressive chemical environments. They also show a high potential for using recycled targets in their manufacturing. This paper analyzes the fresh and cured properties of polyester polymer concretes containing two metallurgical wastes, namely: ladle slag and alumina filler. Both targets require a higher resin dosage than sand. The standard consistency test showed a low representativeness of the recycled fresh mixes' workability. The ladle slag and alumina filler samples showed a higher length plastic shrinkage than those containing sand. All of the targets obtained cured density values in the range of 1.589–1.912 g/cm³. From a mechanical point of view, the sand and alumina filler containing polyester polymer concretes reached 11.02 and 10.93 kN, respectively, of flexural strength, while the ladle slag samples showed the best result with 19.31 kN. In the compressive strength test, the sand and alumina filler combinations reached 106.16 and 104.21 MPa, respectively, while the ladle slag achieved 160.48 MPa. The flexural and compressive elasticity modulus showed similar trends related to the resin content.

Keywords: polymer concrete; resin; polyester; metallurgical waste; recycled target

1. Introduction

Polyester polymer concretes (PPCs) are composite materials made up of organic resins as a binder, and aggregates or fillers as the target materials. These composite materials develop, by means of exothermic chemical reactions with hardeners and accelerators, a continuous resistant polymer matrix around the target particles. PPCs have been receiving increasing interest in recent years because of their good characteristics compared with traditional concrete, namely: improved mechanical strength, superior durability, good resistance to water, lower permeability, high chemical and corrosion resistances, excellent adhesion and a fast curing process, among others [1,2]. However, PPCs also show some disadvantages, like a lower workability, fresh resin odor, lower resistance to high temperatures, and higher cost compared with conventional concrete [3]. An effective way to decrease these shortcomings, in agreement with the actual environmentally friendly thinking trends, consists of using recycled targets instead of raw materials for PPC manufacturing. PPCs show a high potential for the

incorporation of recycled materials because of the nature of their polymer matrix and their lack of bonds with the target particles [4]. In addition, the use of recycled targets for PPC manufacturing could suppose an effective method of valorization for large quantities of different wastes. This could not only improve the sustainability of the resulting PPC products, but also the natural resources preservation, in accordance with the circular economy principles [5]. Different applications could benefit from the use of PPC-containing recycled target materials, mainly those that are not subject to strict structural concrete regulations. Nevertheless, not all wastes have the same potential for PPC manufacturing, as their own characteristics can modify the fresh or final product properties. Extensive research works have been conducted for determining the properties of PPCs made up of different recycled targets, like aggregates, sand, clay, fillers, fly ash, fuel ashes, plastics, or recycled fiber reinforced polymers, among others [1,3,4,6–13]. However, nowadays, huge amounts of different wastes, with potential as PPC targets, continue to be disposed in landfills around the world and pollute the environment. Based on their good properties as aggregates for conventional concrete manufacturing, one of the most promising is metallurgical wastes [14–17]. Nonetheless, there is a lack of knowledge about the ability of these materials as PPC components. Thus, this study analyzes the aptitude of two metallurgical wastes as target materials for PPC manufacturing—alumina filler (AF) and ladle slags (LS). Large quantities of both wastes are continuously generated, and because of the lack of effective valorization methods, high volumes are available around the world. Their use for PPC manufacturing would have important environmental and economic advantages for waste producers and PPC manufacturing companies. Under these environmental and economic considerations, an experimental laboratory investigation was carried out. Its aim was to develop the knowledge—which is currently not available—between these non-conventional target materials and the fresh and mechanical properties of polyester polymer concrete.

2. Materials and Methods

2.1. Materials

The resin used in this work was an unsaturated orthoitaic tixotropic non-accelerated polyester mixture known as CRYSTIC 406 NT. This product was specifically developed for PPC manufacturing based on its chemical and mechanical features, as well as its lower cost compared with other resins. This resin contains ultra-violet absorbents that provide good resistance against solar radiation. Its low viscosity and quick setting time allow for a high production efficiency. The polyester mixture comprises two parts that are supplied separately, namely: the resin itself and an accelerator based on cobalt salts and metiletilketone peroxide as the catalyzer. Table 1 shows the main liquid and cured characteristics of this resin.

Table 1. Polyester CRYSTIC 406 NT liquid and cured resin characteristics.

Characteristic	Units	Value
Liquid resin		
Viscosity at 25 °C	dPas	3.5–4.5
Specific gravity	g/cm ³	1.10
Volatile content	%	36–40
Acidity index	mg KOH/g	19–23
Cured resin		
Deformation temperature under load	°C	65
Absorption after 24 h of immersion in water	mg	15

AF is generated as a secondary waste during the valorization of alumina salt slags that are produced during the alumina recycling process. Around 110,000 tonnes of AF waste is generated per year in Spain. LSs are also called secondary refining or white slags. They are produced when the steel is desulfurized in the transport ladle during iron or steel making from scrap-iron in electric arc

furnaces. The yearly Spanish production of LS exceeds 340,000 tonnes. A siliceous sand from siliceous rock crushing was used as a reference target for the sample manufacturing.

Figure 1 shows the granulometric curves of the different target materials used in this investigation. Table 2 shows their chemical composition, expressed as the main oxides, obtained by X-ray fluorescence (XRF), and the mineralogical composition, which is estimated by X-ray diffraction (XRD) analysis.

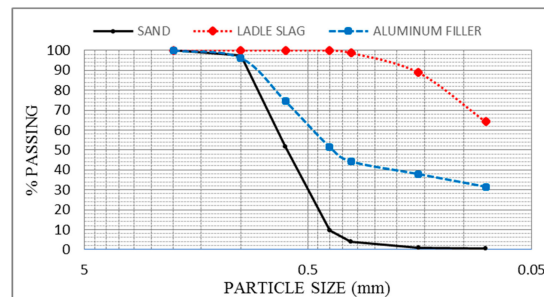
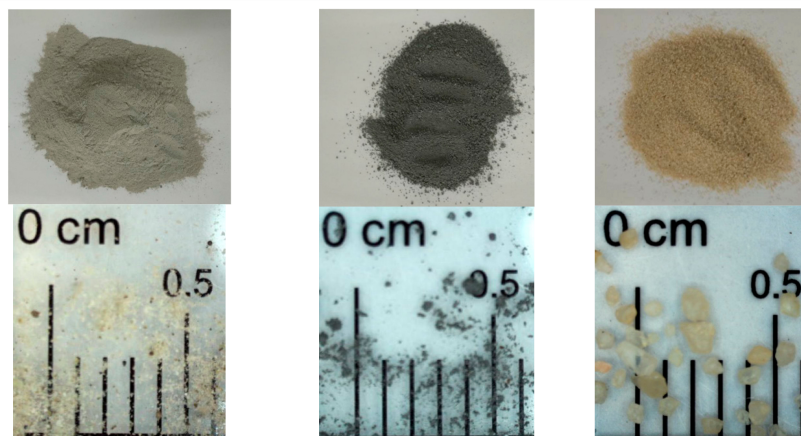


Figure 1. Granulometric curves of the target materials.

Table 2. Chemical, mineralogical, and physical characterization of the target materials.

Chemical Composition					
Ladle Slag		Alumina Filler		Sand	
Oxides	(%)	Oxides	(%)	Oxides	(%)
CaO	57	Al ₂ O ₃	64		
SiO ₂	21	MgO	7	SiO ₂	98
Al ₂ O ₃	7	SiO ₂	7	Al ₂ O ₃	1
MgO	6	CaO	2		
F	5	Na ₂ O	2		
SO ₃	2	F	1		
Fe ₂ O ₃	1	Fe ₂ O ₃	1		
Mineralogical Composition					
Periclase		Gibbsite		Quartz	
Olivine		Nordstrandite			
Calcium silicate oxide		Aluminum oxide			
Calcium silicate					
Calcium aluminum oxide fluoride					
Calcium silicate oxide					
1.372		Bulk Density (g/cm ³)		1.531	
		1.094			
64.23		Particles Under 80 μ (%)		0.58	
		31.40			
2.5 Y 7/1		Color (based on the Munsell Soil Color Chart)		2.5 Y 7/4	
		2.5 Y 5/1			
		Alkali-Silica Reaction (UNE 146512) [18]			
Not reactive		Not reactive		Not reactive	



2.2. Methods

For the sample manufacturing, the resin and target were carefully mixed using an electrical mixing drill for five minutes. The catalyzer was then added, and the mix was mixed again for an additional five minutes in order to guarantee complete homogenization. After that, the mixture was filled in prismatic $40 \times 40 \times 160$ mm molds coated with a mold-release agent. The fresh samples were vibrated to eliminate air, as well as for the correct filling of the molds. The samples were prepared by changing the resin content by 5% in the mass of the total sample, to state the optimum resin dosage range for each target. After preparation, the samples were maintained at room conditions for 1 h before demolding. A 24 h cure in an oven at 40 °C was carried out to guarantee the complete polymerization of the resin and the curing homogeneity of all of the samples. Finally, the samples were maintained at room temperature for seven days before testing. Each combination was encoded by letters that identified the aggregate type (S for sand, LS for the ladle slag, and AF for alumina filler), followed by the resin content, expressed as a mass percentage of the total mix. Samples with no target materials were manufactured as a reference and were identified as resin.

Because of the lack of specific standardized tests for PPC characterization, and considering the target material particles' size, conventional mortars tests, in accordance with European standards, were considered for the PPC characterization. Thus, the following properties were considered: (i) fresh characteristics, (ii) cured physical properties, and (iii) mechanical strength. Table 3 shows the tests carried out and the reference standards.

Table 3. Laboratory investigation tests.

Characteristic Categories	Tests	Reference Standard
Fresh characteristics	Resin content limits	-
	Fresh consistency	EN 1015-3 [19]
Cured physical properties	Retraction	EN 12390-1 [20]
	Density	EN 12390-7 [21]
Mechanical strength	Flexural strength	EN 12390-5 [22]
	Flexural modulus of elasticity	EN 12390-5 [22]
	Compressive strength	EN 12390-13 [23]
	Compressive modulus of elasticity	EN 12390-3 [24]

The highest resin content limit was defined based on the observed excess of resin on the upper surface of the samples after vibrating. On the other hand, the workability needs for the fresh samples' mixing, molding, and vibration were considered to show the lowest limit of the resin optimum content. A fresh consistency test was carried out in a flow table in accordance with the EN 1015-3 [19] standard. The plastic shrinkage and density were stated in accordance with the EN 12390-1 [20] and EN 12390-7 [21], respectively. The flexural strength and flexural modulus of the elasticity were obtained in accordance with EN 12390-5 [22]. Finally, the compressive strength and compressive modulus of the elasticity tests were carried out, based on the procedure of standards EN 12390-13 [23] and EN 12390-3 [24], respectively.

3. Results and Discussion

3.1. Fresh Physical Characteristics

Figure 2 shows the fresh consistency variations of the fresh mixes for each target material in its optimum resin dosage range. Considering the workability criterion, the sand samples required a dosage above 20% resin, while the LS and the AF samples' workability started with a minimum resin content of 35%. The excess of resin was observed for dosages above 30% in the case of sand, and 45% for the LS and AF combinations. The higher resin content required for the LS and AF samples is probably related to the high content of these materials in the finest particles, which are 66.23% and

31.40% under 80 μ , respectively. The fresh consistency test expresses the combinations consistency as the “cake diameter” of the fresh PPC sample after a shaking process, defined in the European Standard EN 1015-3 [19].

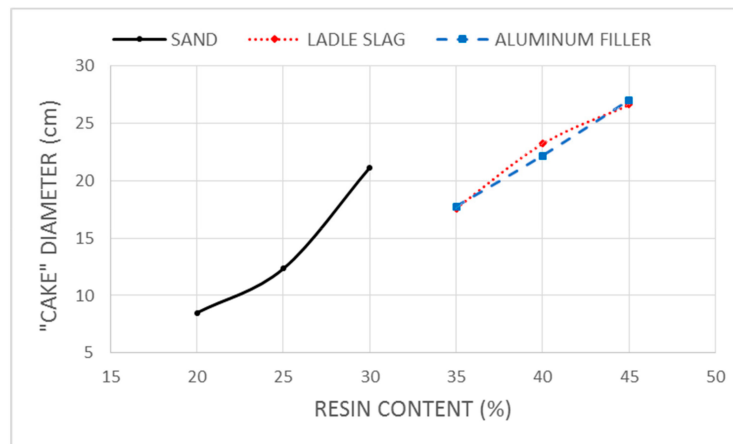


Figure 2. Resin dosage intervals and consistency test results.

For the three target materials, the highest consistencies, corresponding to the lowest cake diameters, were observed at the lowest resin dosages. Thus, the S-20 combination reached a consistency of 8.5 cm, LS-35 reached 17.6 cm, and AF-35 reached 17.7 cm. In all of the cases, the mixes’ workability improved as the resin content increased. Thus, the S-25 combination diameter increased until 12.4 cm, LS-40 until 23.3 cm, and AF-40 until 22.2 cm. As expected, the lowest consistencies were obtained for the highest resin dosages, namely: 21.1 cm for the S-30 combination, 26.6 cm for the LS-40, and 27.0 cm for the AF-40. It is noticeable that although sand requires a lower resin content, it showed a lower workability than LS and AF, which obtained very close consistencies. These results demonstrated that, as well as the resin dosage range, the fresh PPC consistency depends on the existence of a minimum content of finest particles, which strongly control the fresh mix rheology.

3.2. Cured Physical Properties

Figure 3 shows the length plastic shrinkage results of the different combinations tested after the curing period.

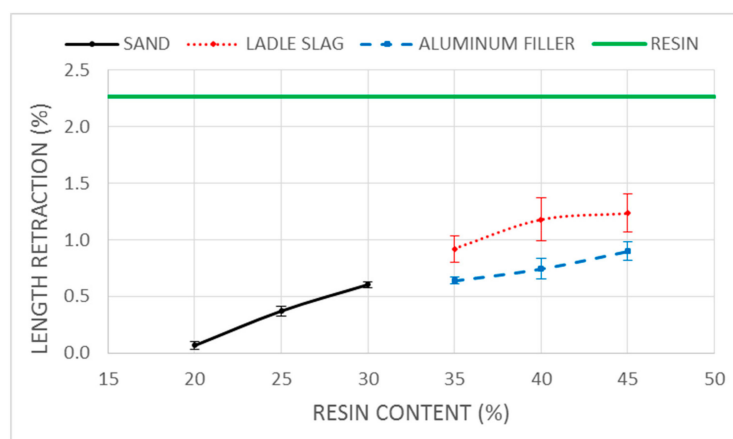


Figure 3. Length retraction test results.

The pure resin results for all of the following tests are depicted as a continuous line as a reference. In this case, the resin plastic shrinkage was 2.263%. The sample plastic shrinkages were lower than the control resin value, and showed a direct relationship with the resin content. The lowest length plastic

shrinkage values were obtained in the sand combinations within the 0.067%–0.604% range, probably due to the lower resin dosages needed for this target. Sand also showed the lowest result variability, with standard deviations (σ) between 0.026 and 0.044. The highest length plastic shrinkages and variability values were obtained by the LS combinations with ranges of 0.917%–1.235% and 0.118–0.191, respectively. Finally, the AF samples reached plastic shrinkages between 0.640% and 0.898% with σ values between 0.031 and 0.088. This test shows the importance of the use of target materials for the PPC length plastic shrinkage decrease, because of the reduction of resin content in the PPC. The length plastic shrinkage differences and the results' variability highlights the influence of the target granulometry in this PPC characteristic.

The cured PPC densities are shown in Figure 4. An increase in the sample densities was observed from 1.220 g/cm³, corresponding to the resin, until 1.870–1.912 g/cm³ for the sand, until 1.749–1.902 g/cm³ for the LS, and until 1.589–1.749 g/cm³ in the case of the AF combinations. The sand samples showed very low-density differences for the different resin dosages, with a maximum observed density of 1.912 g/cm³ for the 25% resin dosage. On the other hand, AF and LS showed an indirect relationship between the samples' cured densities and the resin content. Thus, the LS densities varied between 1.749 g/cm³ for the LS-45 combination and 1.902 g/cm³ for LS-35, and the AF samples varied between 1.589 g/cm³ for AF-45 and 1.749 g/cm³ for AF-35. The sample densities showed, in general, low standard deviations (σ) in the range of 0.007–0.016 for the sand, 0.004–0.013 for the LS, and 0.008–0.030 for the AF. Different density relationship trends were observed between the sand, as well as between the LS and AF resin content combinations. This suggests that the resin does not only fill the interparticle pores, but also produces a partial substitution of target particles, thus decreasing the sample density. This highlights the complexity of the relationship between the bulk target material densities, their particle sizes, the optimum mixes resin dosage ranges, and the PPC densities.

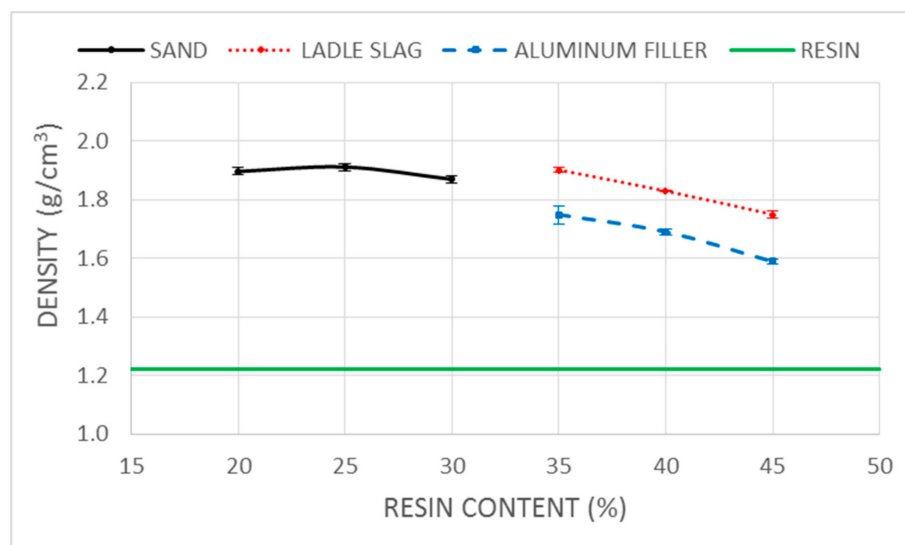


Figure 4. Polyester polymer concretes (PPC) densities.

3.3. Mechanical Strength

Figures 5 and 6 show the flexural maximum load (kN) and the flexural modulus of elasticity (GPa), respectively, based on the three-point test, in accordance with the European Standard EN 12390-5 [22].

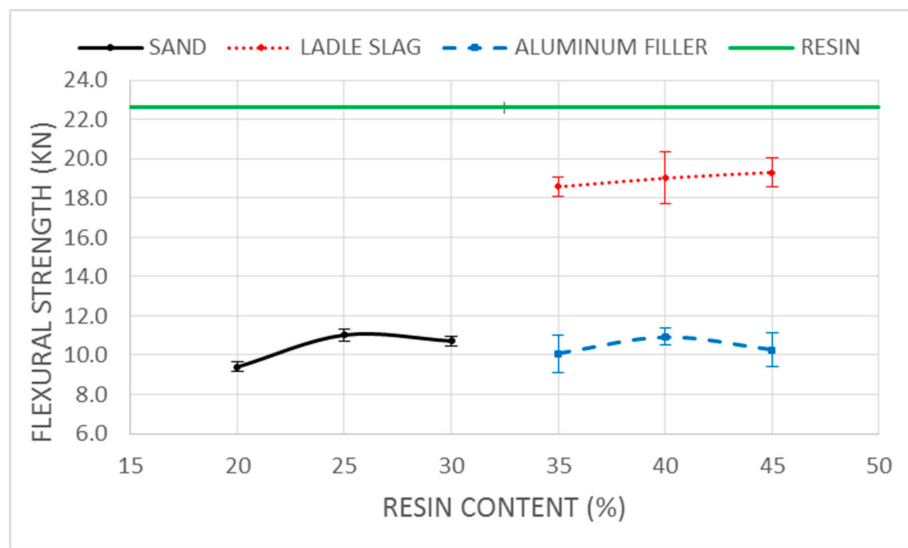


Figure 5. PPC flexural strength.

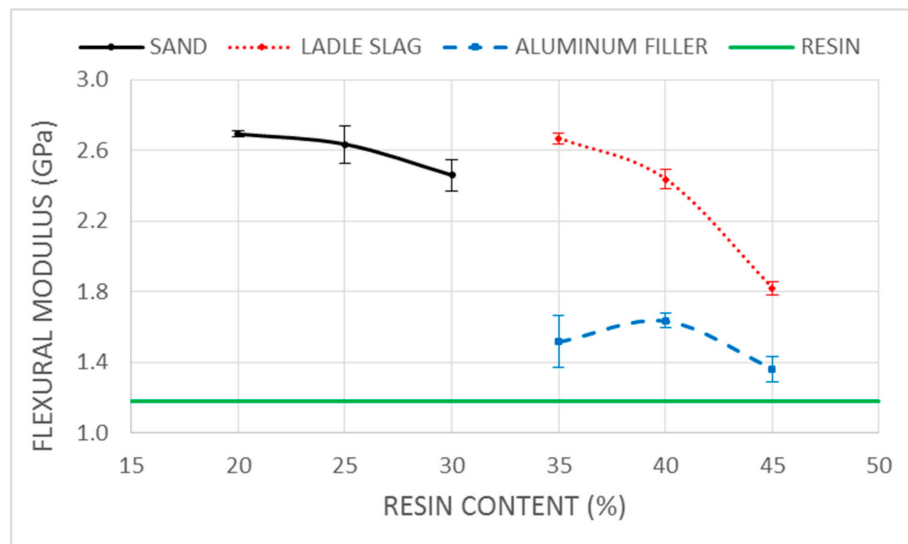


Figure 6. PPC flexural elasticity modulus.

Pure resin showed a flexural strength of 22.61 kN, with $\sigma = 0.002$. For all of the PPC combinations, the flexural strength of the samples was lower than the reference. The sand and AF combinations obtained the lowest values, in the range of 9.40–11.02 kN with σ values of 0.255–0.299, and 10.07–10.93 kN with σ values of 0.434–0.961, respectively. On the other hand, the LS samples achieved flexural strength results of 18.57–19.31 kN with σ values of 0.494–1.322. This demonstrated that, based on the resin and the target materials, the flexibility of the samples depends on the resin content. However, these results also show some apparent contradictions, namely: (i) the sand and AF combinations achieved close flexural strength results at different resin dosages; (ii) considering the average results and their uncertainty, not one of the target materials showed a direct relationship between the samples' flexibility and the resin content; and (iii) the LS combinations, containing the same resin dosages as the AF, showed a very different flexural strength. These results highlight the importance of the resin matrix surrounding the target particles, which constitutes the PPC-resistant skeleton, and act as breaking points. The flexural modulus of the elasticity demonstrated the flexibility of the resin structure, which became more rigid with the use of target materials in the PPC combinations. The use of targets increased the resin flexural modulus of the elasticity from 1.36 GPa up to 2.45–2.69 GPa for the sand, 1.82–2.67 GPa for the LS, and 1.36–1.63 GPa for the AF combinations. The sand and LS

samples showed an indirect relationship between the resin content and the flexural modulus of the elasticity mean, while in the case of AF, this relationship was not evident, probably because of the AF-35 combination’s larger uncertainty compared with the other samples: The sand combinations’ σ value varied in the range of 0.015 and 0.106, while AF ranged between 0.042 and 0.147, and LS between 0.030 and 0.055.

Figures 7 and 8 show the compressive strength and compressive modulus of the tested combinations, respectively.

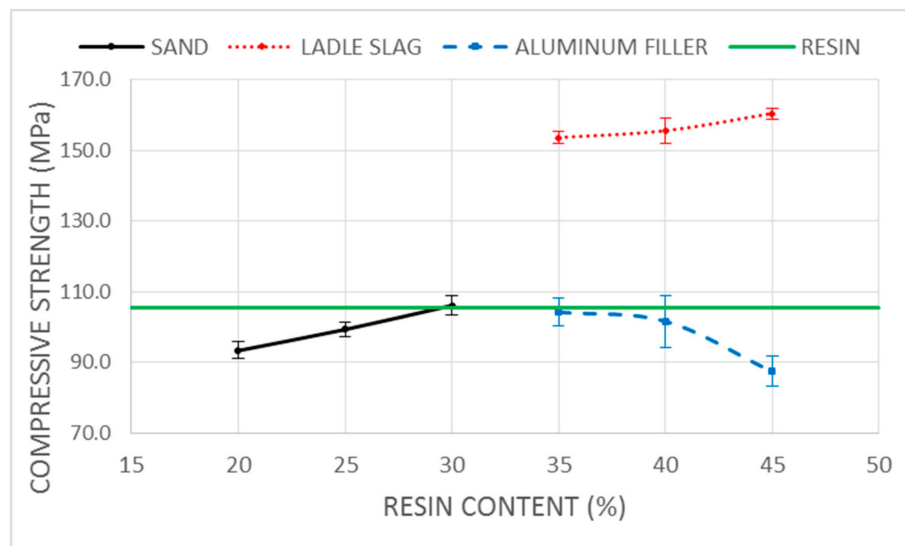


Figure 7. PPC compressive strength.

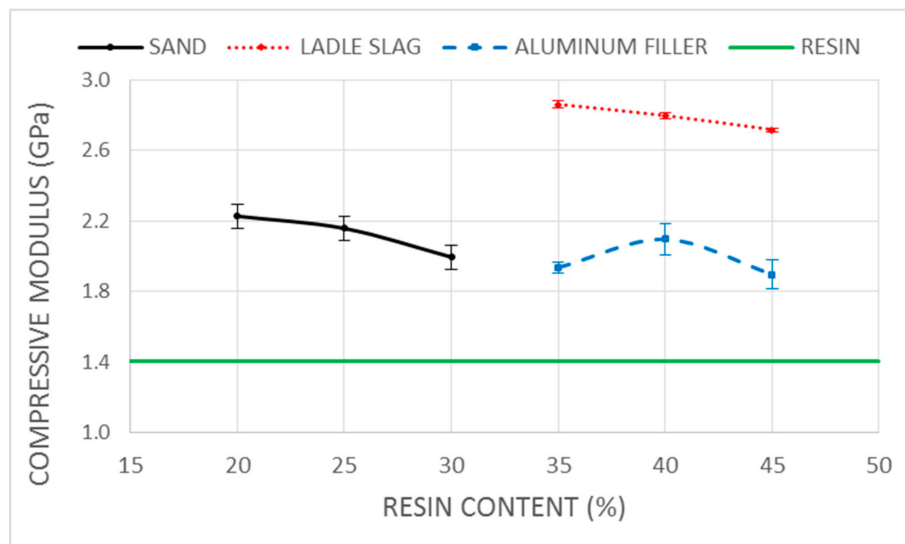


Figure 8. PPC compressive elasticity modulus.

The resin reached 105.31 MPa with a σ value of 4.208. The S-30 combination obtained a very close value of 106.16 MPa, with a σ value of 2.619. For this target, as the resin dosage decreased, the compressive strength also decreased, reaching a value of 93.35 MPa with a σ value of 2.405 for the S-20 combination. The S-25 combination reached an intermediate result of 99.34 MPa, with a σ value of 1.938. On the other hand, the AF combinations showed an apparent decrease of compressive strength as the sample resin content increased, although this indirect relationship cannot accurately be stated, because of the relatively large uncertainties obtained in these target samples. Thus, the combination of AF-35 reached 104.21 MPa with a σ value of 3.852, while AF-40 decreased to 101.61 MPa with a σ

value of 7.285, and AF-45 obtained the lowest compressive strength with 87.42 MPa, with a σ value of 4.282. Finally, the LS combinations obtained compressive strength results that increased by 50% of those obtained with the resin and the other targets samples: the combination LS-35 got 156.67 MPa with a σ value of 1.720, LS-40 obtained 155.60 MPa with a σ value of 3.438, and LS-45 reached the highest compressive strength with 160.48 MPa with a σ value of 1.576. These results highlight, as it was observed in the flexural strength test, the complexity of the relationships between the resin content and the target granulometry in the strength properties of the PPC samples.

The compressive modulus of elasticity showed close patterns to those obtained for the flexural modulus, as follows: (i) in all of the cases, the use of target materials increased the compressive modulus of elasticity compared with the pure resin samples; (ii) the sand and LS combinations showed an indirect relationship between the compressive modulus of elasticity and the resin dosage; and (iii) the AF-40 combination showed the highest compressive modulus of elasticity of this target. In this test, the resin reached 1.40 GPa with a σ value of 0.321. The sand combinations reached 2.23 GPa with a σ value of 0.031 for the S-20, 2.16 GPa with a σ value of 0.013 for the S-25, and 2.00 GPa with a σ value of 0.077 for the S-30 combination. The AF combinations reached 1.94 GPa with a σ value of 0.074 for the AF-35, 2.10 GPa with a σ value of 0.361 for the AF-40, and 1.90 GPa with a σ value of 0.117 for the AF-45 combination. Finally, the highest compressive modulus of elasticity and the lowest uncertainties corresponded to the LS combinations, which obtained 2.86 GPa with a σ value of 0.022 for the LS-35, 2.80 GPa with a σ value of 0.020 for the LS-40, and 2.72 GPa with a σ value of 0.011 for the LS-45 combination.

4. Conclusions

The experimental investigation carried out allowed for drawing the following conclusions, which can help to mitigate the lack of knowledge about the use of metallurgical wastes in the manufacturing of more environmentally friendly PPC.

1. Nonconventional targets required a higher resin dosage than sand to reach the workability required for the manufacturing process, due to their high content of fine particles.
2. Nonconventional targets showed higher length plastic shrinkages compared with those of sand, but maintained it under pure a resin value.
3. The PPC manufactured densities depended on the target materials' bulk densities and granulometries. They both determine the interparticles' pore size and condition the resin dosage required for the workability of fresh mixes, as resin can partially replace fine target particles.
4. In general, the mechanical properties of the nonconventional targets were adequate, as AF obtained close results to those obtained by the sand sample, while LS combinations clearly overcame them, for the flexural strength as well as for the compressive strength tests.

These results allow for stating the potential of these metallurgical wastes, especially of LS, for the replacement of natural targets for more sustainable PPC production. However, some apparently contradictory results were obtained that highlight the need for more investigations of these promising recycled target materials for PPC commercial products manufacturing.

Author Contributions: Conceptualization, A.M.E. and A.S.; methodology, A.S. and S.E.; validation, S.M. and B.G.; formal analysis, S.E.; investigation, B.G.; resources, A.M.E.; data curation, S.M.; writing (original draft preparation), A.S.; writing (review and editing), A.S.; visualization, S.E.; supervision, A.S.; project administration, S.M.; funding acquisition, A.M.E. All authors have read and agreed to the published version of the manuscript.

Funding: This research was funded by Gobierno de Navarra and Fondo Europeo de Desarrollo Regional (FEDER) grant number [0011-1365-2017-000176] And The APC was funded by the Institute of Smart Cities of the Public University of Navarre.

Acknowledgments: The authors acknowledge Gobierno de Navarra, Fondo Europeo de Desarrollo Regional and Institute of Smart Cities of the Public University of Navarre their support on this project.

Conflicts of Interest: The authors declare no conflict of interest.

References

1. Ferdous, W.; Manalo, A.; Aravinthan, T.; Van Erp, G. Properties of epoxy polymer concrete matrix: Effect of resin-to-filler ratio and determination of optimal mix for composite railway sleepers. *Constr. Build. Mater.* **2016**, *124*, 287–300. [[CrossRef](#)]
2. Toufigh, V.; Hosseinali, M.; Shirkhorshidi, S.M. Experimental study and constitutive modeling of polymer concrete's behavior in compression. *Constr. Build. Mater.* **2016**, *112*, 183–190. [[CrossRef](#)]
3. Bulut, H.A.; Şahin, R. A study on mechanical properties of polymer concrete containing electronic plastic waste. *Compos. Struct.* **2017**, *178*, 50–62. [[CrossRef](#)]
4. Ribeiro, M.C.S.; Meira-Castro, A.C.; Silva, F.G.; Santos, J.; Meixedo, J.P.; Fiúza, A.; Dinis, M.L.; Alvim, M.R. Re-use assessment of thermoset composite wastes as aggregate and filler replacement for concrete-polymer composite materials: A case study regarding GFRP pultrusion wastes. *Resour. Conserv. Recycl.* **2015**, *104*, 417–426. [[CrossRef](#)]
5. Commission, E. *CDW: Material Recovery & Backfilling*; European Commission: Brussels, Belgium, 2011.
6. Barbuta, M.; Rujan, M.; Nicuta, A. Characterization of Polymer Concrete with Different Wastes Additions. *Procedia Technol.* **2016**, *22*, 407–412. [[CrossRef](#)]
7. Martínez-Barrera, G.; Menchaca-Campos, C.; Gencel, O. Polyester polymer concrete: Effect of the marble particle sizes and high gamma radiation doses. *Constr. Build. Mater.* **2013**, *41*, 204–208. [[CrossRef](#)]
8. Saribiyik, M.; Piskin, A.; Saribiyik, A. The effects of waste glass powder usage on polymer concrete properties. *Constr. Build. Mater.* **2013**, *47*, 840–844. [[CrossRef](#)]
9. Hong, S.; Kim, H.; Park, S.K. Optimal mix and freeze-thaw durability of polysulfide polymer concrete. *Constr. Build. Mater.* **2016**, *127*, 539–545. [[CrossRef](#)]
10. Khalid, N.H.A.; Hussin, M.W.; Mirza, J.; Ariffin, N.F.; Ismail, M.A.; Lee, H.S.; Mohamed, A.; Jaya, R.P. Palm oil fuel ash as potential green micro-filler in polymer concrete. *Constr. Build. Mater.* **2016**, *102*, 950–960. [[CrossRef](#)]
11. Lokuge, W.P.; Aravinthan, T. Mechanical Properties of Polymer Concrete With Different Types of Resin. In Proceedings of the 22nd Australasian Conference on the Mechanics of Structures and Materials (ACMSM 22), Sydney, Australia, 11–14 December 2012; pp. 1–6.
12. Wang, J.; Dai, Q.; Guo, S.; Si, R. Mechanical and durability performance evaluation of crumb rubber-modified epoxy polymer concrete overlays. *Constr. Build. Mater.* **2019**, *203*, 469–480. [[CrossRef](#)]
13. Sosoi, G.; Barbuta, M.; Serbanoiu, A.A.; Babor, D.; Burlacu, A. Wastes as aggregate substitution in polymer concrete. *Procedia Manuf.* **2018**, *22*, 347–351. [[CrossRef](#)]
14. Lam, M.N.T.; Le, D.H.; Jaritngam, S. Compressive strength and durability properties of roller-compacted concrete pavement containing electric arc furnace slag aggregate and fly ash. *Constr. Build. Mater.* **2018**, *191*, 912–922. [[CrossRef](#)]
15. Guo, Y.; Xie, J.; Zhao, J.; Zuo, K. Utilization of unprocessed steel slag as fine aggregate in normal- and high-strength concrete. *Constr. Build. Mater.* **2019**, *204*, 41–49. [[CrossRef](#)]
16. Sun, J.; Feng, J.; Chen, Z. Effect of ferronickel slag as fine aggregate on properties of concrete. *Constr. Build. Mater.* **2019**, *206*, 201–209. [[CrossRef](#)]
17. Cardoso, C.; Camões, A.; Eires, R.; Mota, A.; Araújo, J.; Castro, F.; Carvalho, J. Using foundry slag of ferrous metals as fine aggregate for concrete. *Resour. Conserv. Recycl.* **2018**, *138*, 130–141. [[CrossRef](#)]
18. AENOR UNE 146512:2018. *Test for Aggregates. Determination of the Potential Reactivity of Aggregates. Chemical Method. Determination of the Reactivity Alkali-Silica and Alkali-Silicate*; Asociación Española de Normalización: Madrid, Spain, 2018.
19. AENOR UNE-EN 1015-3:2000. *Methods of Test for Mortar for Masonry—Part 3: Determination of Consistence of Fresh Mortar (by Flow Table)*; Asociación Española de Normalización: Madrid, Spain, 2000.
20. AENOR UNE-EN 12390-1:2013. *Testing Hardened Concrete—Part 1: Shape, Dimensions and Other Requirements for Specimens and Moulds*; Asociación Española de Normalización: Madrid, Spain, 2013.
21. AENOR UNE-EN 12390-7:2009. *Testing Hardened Concrete—Part 7: Density of Hardened Concrete*; Asociación Española de Normalización: Madrid, Spain, 2009.
22. AENOR UNE-EN 12390-5. *Testing Hardened Concrete—Part 5: Flexural Strength of Test Specimens*; Asociación Española de Normalización: Madrid, Spain, 2009.

23. AENOR UNE-EN 12390-13:2014. *Testing Hardened Concrete—Part 13: Determination of Secant Modulus of Elasticity in Compression*; Asociación Española de Normalización: Madrid, Spain, 2014.
24. AENOR UNE-EN 12390-3:2009. *Testing Hardened Concrete—Part 3: Compressive Strength of Test Specimens*; Asociación Española de Normalización: Madrid, Spain, 2009.



© 2020 by the authors. Licensee MDPI, Basel, Switzerland. This article is an open access article distributed under the terms and conditions of the Creative Commons Attribution (CC BY) license (<http://creativecommons.org/licenses/by/4.0/>).